

DOI: <http://dx.doi.org/10.21123/bsj.2017.14.3.0539>

Sol- Gel Synthesis of Hematite Nanoparticles and Photo Degradation of Cibacron Red FN-R Dye

*Ahlan M. Farhan** *Hussein I. Abdullah*** *Asmaa J. Ali***

Department of Chemistry, College of Science for Women, University of Baghdad, Baghdad, Iraq.

Department of Chemistry, College of Science, AL-Mustansyriah University, Baghdad, Iraq.

E-mail: asas.jameil@yahoo.com

Received 30/12 /2015

Accepted 3/11 /2016



This work is licensed under a [Creative Commons Attribution 4.0 International License](https://creativecommons.org/licenses/by/4.0/).

Abstract

This paper describes the synthesis of α -Fe₂O₃ nanoparticles by sol-gel route using carboxylic acid(2-hydroxy benzoic acid) as gelatin media and its photo activity for degradation of cibacron red dye . Hematite samples are synthesized at different temperatures: 400, 500, 600, 700, 800 and 900 °C at 700 °C the α -Fe₂O₃ nanoparticles are formed with particle size 71.93 nm. The nanoparticles are characterized by XRD , SEM, AFM and FTIR . The 0.046 g /l of the catalyst sample shows high photo activity at 3×10^{-5} M dye concentration in acidic medium at pH 3.

Key words: Hematite, Sol-Gel Method, Cibacron Red FN-R Dye, Photo Degradation.

Introduction:

Azo dyes are the largest group of dyes with –N=N–, as a chromophore in an aromatic system and have wide application in textile industries due to their ease of synthesis, versatility and cost effectiveness[1,2]. However, due to the strong toxicity and the high solubility of these dyes ,different methods are proposed for their removal such as adsorption, filtration, flocculation and catalytic action [3]. Semiconductor photo catalysis is a quickly organizing multidisciplinary research field with potential applications in mineralization of organic pollutants. The advanced oxidation processes (AOP) have been considered as an effective technology in treating organic

chemicals containing dyes in wastewater [4]. Iron oxides exist in nature in many forms such as hematite (α -Fe₂O₃) , maghemite (γ -Fe₂O₃) and magnetite (Fe₃O₄). Among those phases hematite is one of the most attractive and significant metal oxide [5]. Many methods on the synthesis of iron oxide NPs by sol – gel are developed [6,7]. Tang and his co-workers report the synthesis of α -Fe₂O₃ nanorods through the calcination of Fe OOH nanorods precursor[8] , Zhang *et al.* [9] use the sol – gel route to prepare hematite nanoparticles at various temperatures (423 - 800 K) . The present work describes the synthesis of hematite (α -Fe₂O₃) NPs by sol- gel route using 2-

hydroxy benzoic acid as a gelatin agent and its use in photo degradation of cibacron red dye. The SEM, XRD, AFM, & FTIR technique is used to characterize the hematite nanoparticles.

Materials and Methods:

Material Preparation : Iron oxide nanoparticles are synthesized by sol-gel route using ferric chloride as iron source from SDFCL (97%) analytical grad and 2-hydroxy benzoic acid as a gelatin agent. In a typical synthesis (1.6 g, 9.87 mmole) of ferric chloride is dissolved in distilled water (100 cm³) with stirring for 30 min. to complete dissolution in the same way as we check the pH. On the other hand, (2.7 g, 19.5 mmole) of gelatin is dissolved in a small amount of absolute ethanol (10 cm³) to complete dissolution and then 100 cm³ of distilled water is added with stirring for 30 min. and the mixture is heated at 60 °C for one hour at pH 8 by adding drops of (30%) ammonium hydroxide. The color of solution changes to purple and the solution turns to gel followed by drying in oven at 80 °C for four hours. The obtained compound is calcined at different temperatures for 2 hours using muffle furnace to obtain the product.

Characterizations : The identification phase, particle size and crystalline structure analysis are determined by XRD using Shimadzu -6000 model with a Cu radiation ($\lambda = 1.54 \text{ \AA}$), voltage 40 Kv and current 30 mA with speed 5° / min. The Atomic force microscopy (AFM) CAPM type AA3000 is used to investigate the particle size and morphology of the derived nanoparticles.

Catalytic Activity Test: The photolysis of dyes has been performed using a tungsten lamp (600W). UV-Visible spectral absorption bands are obtained using Shimadzu SPUV-18 spectrophotometer at 25°C. Distilled water is used as solvent and quartz photochemical cell. A known

concentration of the dye solution ($3 \times 10^{-5} \text{ M}$) of Cibacron Red is introduced into the cell and $\alpha\text{-Fe}_2\text{O}_3$ nanoparticles are added (0.046 g/L), 4 drops of 30% H_2O_2 with a continuous magnetically stirred reaction mixture (75 ml) in a photo reactor are irradiated with a visible lamp (600W) for three hours. Two milliliter samples are taken at various irradiation time intervals. The $\alpha\text{-Fe}_2\text{O}_3$ nanoparticles are removed from the samples using centrifugation for 20 minutes and the concentration of dye solutions is analyzed spectrophotometrically (using UV-Vis Spectrophotometer at $\lambda = 541 \text{ nm}$ for Cibacron Red). Another set of experiments has been done at different pH values ranging from pH 3 to pH 11 made up by sodium hydroxide solution (0.1N) NaOH and (0.1N) HCl.

Results and Discussion:

AFM Analysis

Figure (1) shows the AFM images and the corresponding size distributions of the $\alpha\text{-Fe}_2\text{O}_3$ nanoparticles. It is clear from Figure that the average diameter of $\alpha\text{-Fe}_2\text{O}_3$ nanoparticles is 71.93 nm which are observed over the entire surface, as shown in the inset. The 3-dimensional (3D) AFM image of material nanoparticle in which the irregular and randomly distributed, with a maximum value of 0.38 nm exhibits morphology with a root-mean-square (RMS) roughness of 0.077 nm. A number of earlier studies have investigated the surface structure of hematite dispersions characterized by a variability of morphology and particle size from AFM and TEM techniques [10, 11, 12]. Also, the atomic force microscope (AFM) is used to determine nanoparticles size [13, 14, 15]. The analysis of the roughness leads to an average dimension of 71.93 nm. So it can be concluded that it is possible to measure the size distribution of NPs with AFM too but this technique is

bounded because it is very complex with respect to DLS.

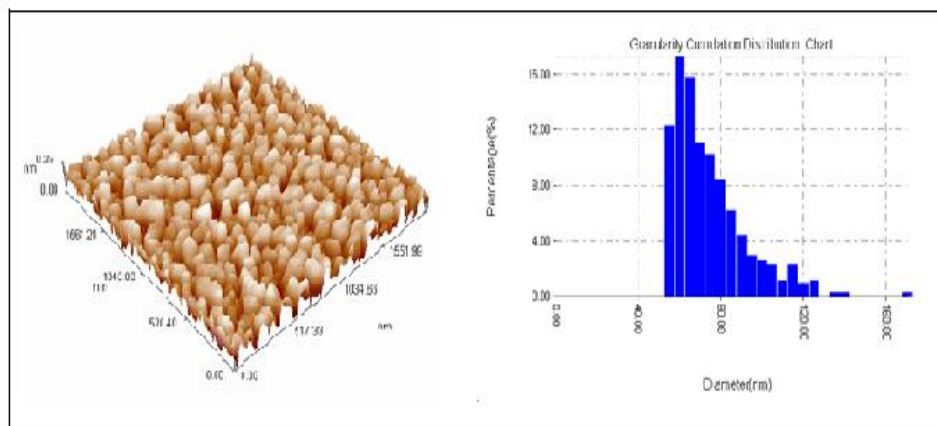
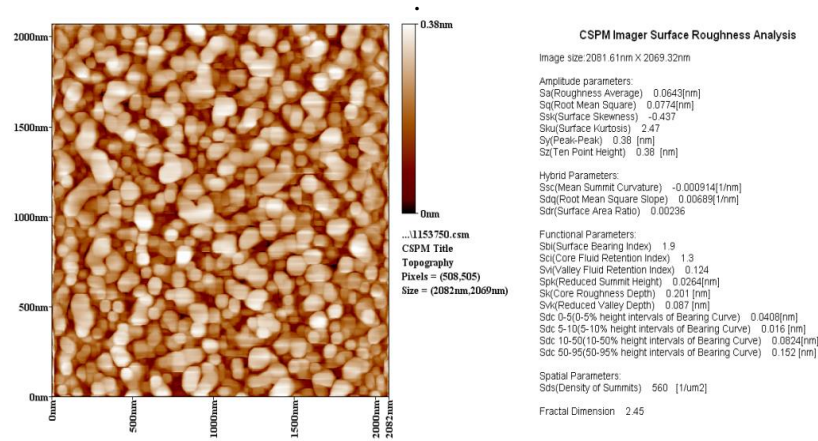


Fig. (1): AFM Images for Nanoparticles Synthesized from 2- Hydroxy Benzoic Acid at 700 °C Calcination through Sol-Gel .

Table (1) shows the decreasing of the particle size with increasing temperature until 700 °C, where particle size increases with increasing temperature.

Table (1): Effect of temperature on the average particle size of $\alpha - Fe_2O_3$ nanoparticles using carboxylic acids (2-hydroxy benzoic acid).

Temperature (°C)	400	500	600	700	800	900
Particle size (nm)	85.40	85.11	72.71	71.93	92.76	94.52

XRD Analysis

The XRD patterns for $\alpha - Fe_2O_3$ nanoparticles (calcined at 700°C for 2 hr.) synthesized by sol–gel method using gelatin as a media and it is explained in Figure (2) .The XRD peaks in the whole angle range of 2 θ from 10° to 70° with Cu radiation ($\lambda= 1.54\text{\AA}$) voltage 40Kv and current 30 mA with speed 5°/min. It can be found from

Figure 2, the XRD patterns are indefinite to pure hexagonal structure the peaks appeared at 2 θ range of (24.2°, 33.2°, 35.6°, 41.1°, 49.5°, 54.1°, 57.4°, 62.4° and 64.0°) can be attributed to the crystalline structures corresponding to pure $\alpha-Fe_2O_3$ nanoparticles. The diffraction peak of the synthesized $\alpha-Fe_2O_3$ are in good agreement with those reported in literatures [16, 17]

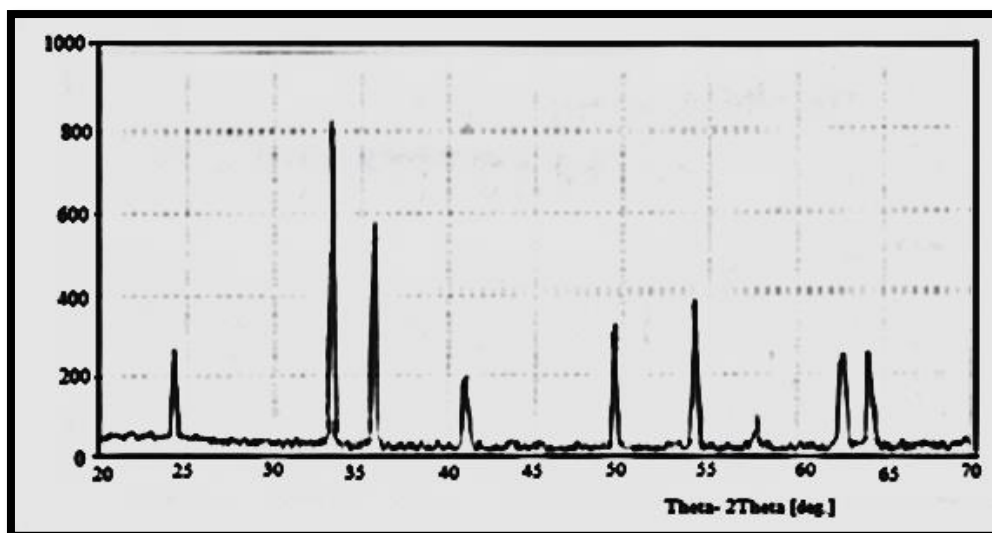


Fig. (2): XRD Patterns of α - Fe_2O_3 Nanoparticles obtained from 2-Hydroxy Phenol after Calcination in 700°C .

FTIR Analysis

FTIR spectra are recorded in the ranges ($400 - 4000\text{ cm}^{-1}$) for the formed complex compound by reacting 2-hydroxy benzoic acid with metals which can be identified by more excellence of their carboxylic and alcoholic (oxy) groups. Figure (3) shows the FTIR spectra of the α - Fe_2O_3 synthesized by sol-gel method assisted by carboxylic acids: 2-hydroxy benzoic acid. It is observed that the bands from the C–O stretching vibrations of the free carboxyl groups are absent. The strong band at 536 and 569 cm^{-1} emerging in IR spectrum of calcined (700°C) compound

shows the presence of stretching and bending vibration of the intercalated M–O species. No peak at the presence of the two intense bands around 1647 and 1436 cm^{-1} indicates the complete replacement of H atoms on the carboxyl groups during the course of the process of complex formation between the carboxylic acid and the ferric ion[18]. The characteristic peak at (455 & 536 cm^{-1}) for 2- benzoic acid becomes very strong, indicating the formation of stretching mode of α - Fe_2O_3 , this specifies the occurrence of hematite nanoparticles in calcined compound.

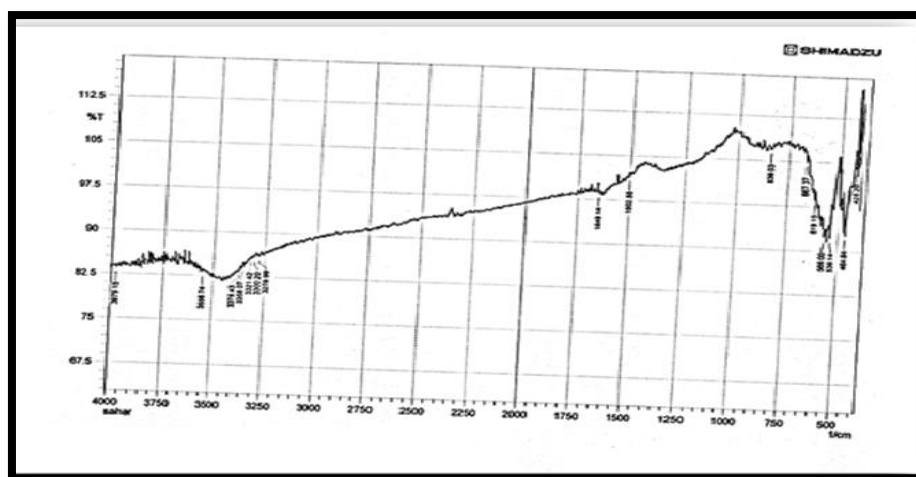


Fig. (3) FTIR Spectra of α - Fe_2O_3 Prepared by Sol-Gel Method using 2- Hydroxy Benzoic Acid after Calcination at 700°C .

Samira Bagheri and co-workers [19] have found strong band at 586 cm^{-1} of calcined 600°C compound showing the presence of stretching and bending vibrations of the intercalated M – O species.

Oxidative Degradation Activity

Test: Figure (4) shows the UV-Visible spectra evolution and degradation efficiency of cibacron red dye (C.B) catalyzed by the- Fe_2O_3 NPs, with the catalytic reaction processing, the intensity of the characteristic peak of C.B decreased gradually after 3 hrs. indicating that 77.81% C.B has been degraded. The high catalytic activity might be attributed to the high specific surface area and the active absorbed oxygen species .The effect of dye concentration on photo degradation of

C.B dye is studied as shown in Figure 5 and Table 2 .The rate of photo degradation is found to increase with increasing dye concentration up to $(3 \times 10^{-5}\text{M})$ due to the availability of more dye molecules for degradation at further increasing in dye concentration,(above $3 \times 10^{-5}\text{ M}$),the rate of photo degradation decreases, An explanation to this behavior is at high dye concentration the path length of incident light which entering the solution decreases which retards the photo on the catalyst surface [20, 21]. Abdullah, R. M. [22] studied the effect of titanium dioxide on some gram negative bacteria and study their effects on some virulence factors and chromosomal DNA.

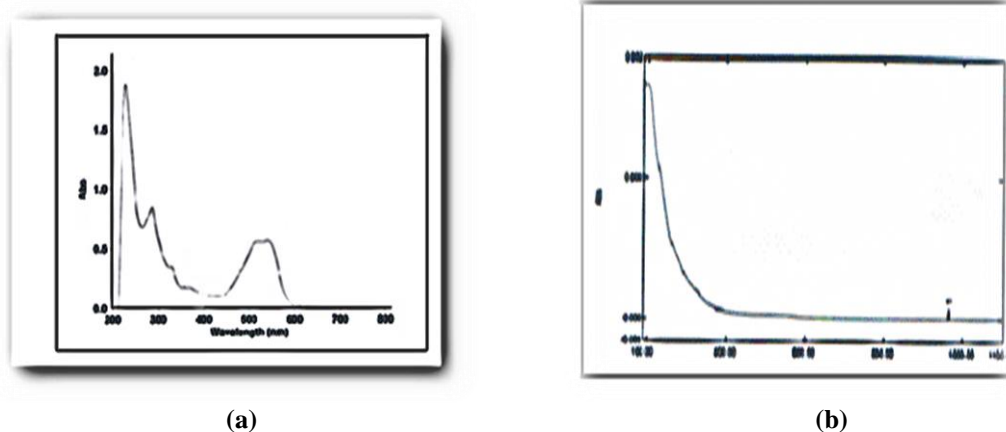
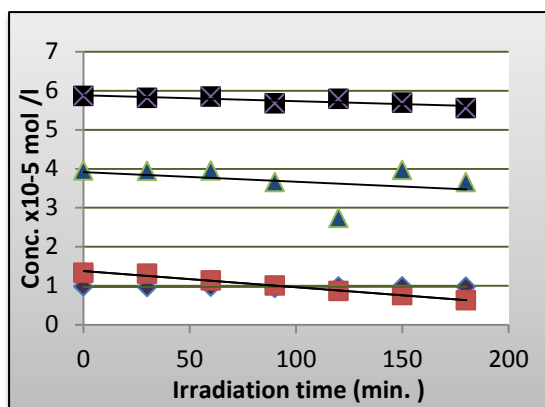


Fig. (4): UV-Visible Spectra for Cibacron Red FN-R (a) Before Irradiation (b) After Irradiation.

Table (2): The Photo Degradation of Cibacron Red Dye at Different Concentration when NPs loading [0.046 g/l]and 30% H_2O_2 at 298K.

[dye]= $1 \times 10^{-5}\text{M}$ +nano+ H_2O_2 +Visible (600W)			[dye]= $3 \times 10^{-5}\text{M}$ +nano+ H_2O_2 +Visible (600W)	
Time (min.)	Absorbance	[Conc.] $\times 10^{-5}\text{M}$	Absorbance	[Conc.] $\times 10^{-5}\text{M}$
0	0.201	0.980	0.273	1.331
30	0.199	0.975	0.240	1.175
60	0.1995	0.973	0.215	1.049
90	0.198	0.969	0.186	0.909
120	0.198	0.967	0.178	0.868
150	0.197	0.961	0.155	0.756
180	0.198	0.967	0.129	0.629
[dye]= $5 \times 10^{-5}\text{M}$ +nano+ H_2O_2 +Visible (600W)			[dye]= $7 \times 10^{-5}\text{M}$ +nano+ H_2O_2 +Visible (600W)	
Time (min.)	Absorbance	[Conc.] $\times 10^{-5}\text{M}$	Absorbance	[Conc.] $\times 10^{-5}\text{M}$
0	0.440	2.146	1.203	5.868
30	0.409	1.995	1.192	5.814
60	0.409	1.995	1.200	5.853
90	0.371	1.809	1.164	5.678
120	0.334	1.629	1.188	5.795
150	0.302	1.473	1.167	5.692
180	0.304	1.482	1.138	5.551



(—●—) $1 \times 10^{-5} \text{ M}$; (—■—) $3 \times 10^{-5} \text{ M}$; (—▲—) $5 \times 10^{-5} \text{ M}$; (—■—) $7 \times 10^{-5} \text{ M}$

Fig.(5): Effect of Different Concentration of C.B Dye on the Photo Catalytic Using Visible lamp (600W) at $\lambda = 541 \text{ nm}$.

Figure .6 shows the effect of $\alpha\text{-Fe}_2\text{O}_3$ loading (mass) varies in the range of (0.015, 0.031, 0.046 and 0.062 g / l) on the reaction. Kinetics under visible light have been studied. The rate of photo degradation immediately increases with increasing the catalyst concentration from 0.01 to 0.06 g/l. Minimum degradation has been observed, because transmittance of incident visible light at low catalyst concentration [23]. The highest rate of photo degradation of dye has been observed at the catalyst concentration of 0.04 g/l with increasing the concentration above 0.04 g/l, the photo activity decreases. The reason for this decrease in rate of photo degradation of dye due to the decrease in number of surface active sites.

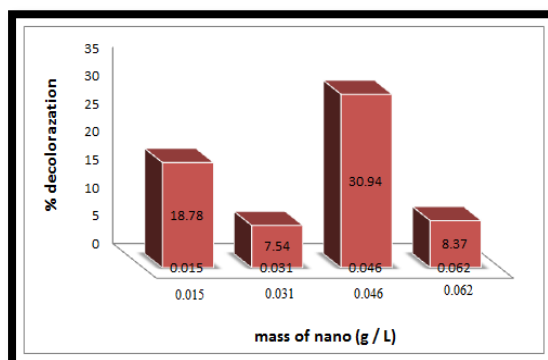


Fig.(6) The Percentage of Decolorization of Dye with Different Catalyst (Nano particles) .

Effect of Medium pH : The effect of variation of pH from 3 to 11 prepared with (0.1N) HCl and (0.1N) NaOH solutions (loading of $\alpha\text{-Fe}_2\text{O}_3$ 0.46 g/ L and initial concentration of dye $3 \times 10^{-5} \text{ M}$) is studied by the photo catalytic degradation of dye .Figure (7) shows increasing of the rate of degradation of dye in acidic medium and decreases in alkaline medium .This may be due to anionic dye particles which get adsorbed on a catalyst surface by exchanging hydroxyl ions from the surface at acidic medium (pH 3) as the concentration of hydrogen ions in dye solution increases. The rate of adsorption and hence the degradation increases.

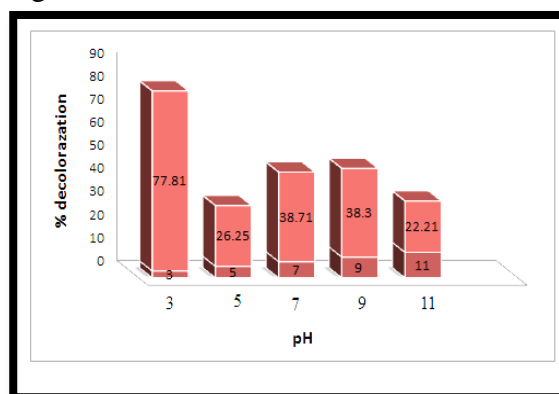


Fig. (7) Effect of Different pH on the Percentage of Decolorization of Cibacron Red Dye.

Conclusion:

The hematite nanoparticles are prepared from metal chloride by the sol gel method followed by calcination at different temperatures. In AFM analysis, the particle size of produced $\alpha\text{-Fe}_2\text{O}_3$ is approximately 71.93 nm and considerably high photo activity about 77.81% of the cibacron red dye decomposed in 3 hr. at catalyst $\alpha\text{-Fe}_2\text{O}_3$ loading of 0.046 g / l.

References:

- [1] Linfeug, Z. and Yuanxin, Wn. 2013. Sol-gel synthesized magnetic MnFe₂O₄ spinel ferrite NPs as novel catalyst for oxidative degradation of

- methyl orange, J. Nanomaterials., 2013, 6 pages.
- [2] Lavanya, C.; Rajeshdhankar; S. and Surita S. 2014. Degradation of toxic dyes:A Review, International. J. Current. Microbiol. Appl. Sci., 3(6):189-199.
- [3] Kajbafvala, A.; Ghorbani, H.; Paravar, A.; Samberg, J. P.; Kajbafvala, E. and Sadrnezhaad, S.K. 2012. Effects of morphology on photocatalytic performance of zinc oxide nanostructures synthesized by rapid microwave irradiation methods, Superlattice Microst, 51 (4):512-522.
- [4] Glaze, W. H. and Kang, J. W. 1989. Advanced oxidation processes, description of a kinetic model for the oxidation of hazardous materials in aqueous media with ozone and hydrogen peroxide in a semibatch reactor, Ind. Eng. Chem. Res., 28,1573.
- [5] Baoliang, I.; Xu, V.Y.; Wu, D. and Sun, Y. 2009. Preparation of α -Fe₂O₃ nano disks by blocking the growth of (001)plane, J. Mater. Sci. Technol., 25(2):155-158.
- [6] Moreau, J. J. E. and Man, M. 1998. The design of selective catalysts from hybrid silica –based materials, Coord. chem. Rev.,178-180,1073-1084.
- [7] Lambert, S. D.; Gommès, C.; Alie, C.; Tcherkassova, N.; Pirard, J. P. and Heinrichs, B. 2005. Formation and structural characteristics of Pd - Ag /SiO₂ and Pd-Cu/SiO₂ catalyst synthesized by cogelation, J.Non-crystalline.Solids., 351(52-54),3839 - 3853.
- [8] Tang, B.; Wang, G.; Zhuo, L.; Ge, J. and Cur, L. 2006. Facile Route to α -FeOOH and α -Fe₂O₃ nanorods and magnetic property of α -Fe₂O₃ nanorods, Inorg. Chem., 45(13): 5196-5200.
- [9] Zhang, Rong Lx, J.; Liu Y. and Bz Dong. 2003. SAXS study on the microstructure of Fe₂O₃ nano crystal, Mat.Sci.Eng.A:351, 224-227.
- [10] Gupta, A. K. and Gupta, M. 2005. Synthesis and surface engineering of iron oxide nanoparticles for biomedical applications, Biomaterials., 26(18):3995-4021.
- [11] Tamdor, R.; Rosens Weig, R. E.; Frey, J. and Klein, J. 2000. Resolving the puzzle of perfluorinated dispersant, Langmuir, 16 (24), 9117-9120.
- [12] Claudio, C.; Giuseppe, P.; Andrea, C.; and Ruggero, A. 2012. Characterization of synthetic hematite (α -Fe₂O₃) nanoparticles using a multi-technique approach, J. Colloid and Interface Sci., 374,118-126.
- [13] Swati, C.; Chandrika, V. and kunal G. 2014. Abinitio studies on hematite surface and the adsorption of phosphate, J. Theoretical chemistry, 2014, 7pages.
- [14] Jingjie, Niu.; Becker, U. and Rodney, E. 2012. In situ AFM and XPS investigation of U⁶⁺ Reduction by Fe²⁺ on hematite and pyrite, J. Materials Res. Society., 1444.
- [15] Eric Balnois and Kevin J. Wilkinson J. 2002. Sample preparation techniques for the observation of environmental biopolymers by atomic force microscopy, Colloid and surface A. physicochemical and Engineering Aspects, 207: 229-242.
- [16] Karthikeyeni S. and Siva Vijaya Kumar T. 2013. Biosynthesis of iron oxide nanoparticles and its haematological effects on fresh water fish oreochromis mossambicus, J. Acad.Indus.Res., 1 (10).
- [17] Shahwan, T.; Abu Sirriah, S.; Nairat, M.; Boyaci, E.; Eroglu, A. E., Scott T. B. and Hallam, K. R. 2011. Green synthesis of iron nanoparticles and their application as a fenton-like catalyst for the degradation of aqueous cationic and anionic dyes, J. Chemical Engineering, 172: 258-266.

- [18] Ermelinda, M. S.; Macôas, Uifaustu R.; Jan Luudell, Petterson, M. and Rasanen, M. 2001. A Matrix isolation spectroscopic and Quantum chemical study of fumaric and maleic acid, J. Phys. chem. A: 105 (15):3922-3933.
- [19] Bagheri, Samira and Sharifah, Bee A. H. 2013. Generation of hematite nanoparticles via sol-gel method, Res. J. Chem. Sci., 3(7): 62-68.
- [20] Hanan Egzar, K.; Mashkour, M. S. and Juda, A. M. 2013. Study the photo degradation of Aniline Blue dye in aqueous phase by using different photo catalysts , ATBAS, 03 (02).
- [21] Umpucho, C. and Sakaew, S. 2013. Removal of methyl orange from aqueous solutions by adsorption using chitosan intercalated montmorillonite, Songkla nakarin. J. Sci. Technol., 35 (4):451-454.
- [22] Abdullah, R. M., 2016. A Study the effect of titanium dioxide nanoparticles combination with antibiotics and plant extracts against some gram negative bacteria., Baghdad Science Journal,13(3):425-434.
- [23] Chen, C.C.; and Lu, C. S. 2007. Mechanistic studies of the photo catalytic degradation of methyl green : an investigation of products of the decomposition processes, Environ.Sci.Technol., 41:4389-4396.

تحضير الهيميتايت النانوية بطريقة السول – جل والتجزئة الضوئية لصبغة سيباكرون الاحمر FN-R

احلام محمد فرحان * حسين اسماعيل عبد الله ** اسماء جميل علي **

*قسم الكيمياء، كلية العلوم للبنات، جامعة بغداد، بغداد، العراق.
**قسم الكيمياء، كلية العلوم، الجامعة المستنصرية، بغداد، العراق.

البريد الالكتروني: asas.jameil@yahoo.com

الخلاصة:

تم في هذا البحث تحضير الدقائق النانوية من الهيميتايت ($\alpha\text{-Fe}_2\text{O}_3$) بطريقة السول- جل بأستخدام حامض كربوكسيل كليناند في درجات حرارية مختلفة (400، 500، 600، 700، 800 و 900 م°) وأستخدم كعامل محفز في عملية التجزئة الضوئية لصبغة سيباكرون الاحمر. ووجد ان حجم الدقائق النانوية عند 700 م° هو 71,93 نانومتر. تم تشخيص الدقائق النانوية المحضرة بالتقنيات الاتية : الاشعة تحت الحمراء: (FTIR)، مجهر القوة الذرية (AFM) والاشعة السينية (XRD). (0,046 غم/لتر) من المحفز اعطى اعلى نسبة للتجزئة الضوئية للصبغة بتركيز (3×10^{-5} مولاري) في وسط حامضي (pH 3).

الكلمات المفتاحية : الهيميتايت، طريقة السول – جل، صبغة سيباكرون الاحمر FN-R، التجزئة الضوئية .